International Journal of Heat and Mass Transfer 52 (2009) 3446–3455

Contents lists available at ScienceDirect

International Journal of Heat and Mass Transfer

journal homepage: www.elsevier.com/locate/ijhmt

Using cognitive computing to extend the range of Grashof number in numerical simulation of natural convection

Abhishek Jain, Deborah A. Kaminski *

Department of Mechanical, Aerospace and Nuclear Engineering, Rensselaer Polytechnic Institute, Troy, New York 12180, United States

ARTICLE INFO

Article history:
Received 6 October 2006
Received in revised form 25 February 2009
Available online 4 May 2009

Keywords:
Fuzzy logic
Enclosed cavity
Conjugate heat transfer
Convergence

ABSTRACT

Natural convection in an enclosed cavity with conjugate effects in the walls was simulated over a broad range of Grashof number and the limits of convergence were investigated. A fuzzy controller was employed to adjust relaxation factors dynamically during code execution. The controller operates with a rule set that mimics human expert decision making on the appropriate choice of relaxation factor. Performance of the controller was compared to that of simulations with fixed relaxation factors. Cases investigated involved conjugate heat transfer in one or more walls of a rectangular cavity. Governing equations of continuity, momentum and energy in laminar flow were solved using a finite difference method. Simulating natural convection is more challenging at higher Grashof numbers and convergence is more difficult to attain. The controller was able to extend the range of convergence in all the cases, typically by 4 orders of magnitude, and in one case, by 6 orders of magnitude.

1. Introduction

Natural convection in enclosed cavities has attracted research because of its industrial applications including reactor design, cryogenic systems, cooling of radioactive waste containers, and solar collectors [1–4]. Iterative methods form the basis of solving simultaneously the continuity, momentum, and energy equations in fluid flow in enclosed cavities and heat transfer associated with it. The SIMPLER algorithm [5], a finite difference iterative procedure, uses simple substitution in order to solve the discretized governing equations of fluid motion, energy, and scalar transport. However as stated in [6], the success of the iterative method in most CFD problems relies on the relaxation of state variables. The optimum relaxation factor depends on the nature of the problem, number of grid points used for discretization, grid spacing, iterative procedure used and other parameters. The optimum relaxation factor cannot be analytically determined. In relaxation methods, the value of the variable to be used for obtaining the solution in the next iteration is the value in the current iteration plus a fraction of the difference between the current value and the predicted value.

All computational fluid mechanics relies on heuristic selection of relaxation factors for success; for example, a typical rule of thumb is to set relaxation factors at 0.9 and lower them if the simulation diverges. Selection of a relaxation factor is a simple heuristic approach. This paper demonstrates that CFD can be dramatically improved by using the more sophisticated heuristic approach embodied in fuzzy logic. By using the example of natural convection in an enclosure with conjugate effects, we will show that converged solutions can be obtained for a much wider range of conditions than the simple choice of a constant relaxation factor.

Research concerned with using soft computing methods such as fuzzy logic or neural networks to aid CFD simulations are limited in number in the literature. Dragojlovic et al. [6] used fuzzy logic to control convergence in a turbulent flow simulation. Iida et al. [7] published a study in which wobbling adaptive control was applied to a CFD simulation of the Benard problem. Studies to improve the convergence of genetic algorithms using fuzzy control have been reported in the literature [8–10]. Xunliang et al. [11] controlled the convergence criteria using fuzzy logic based on the residual ratio of the momentum or energy equation.

The relaxation method discussed in the present work enables and improves convergence by slowing down the update rate of the system matrix coefficients. The iterative scheme used in this work is dependent upon the relaxation factor according to the following equation:

$$\phi'_p = \phi^*_p + \alpha^\phi \left(\frac{\sum a_{nb}\phi_{nb} + b}{a_p} - \phi^*_p \right)$$

where $0 < \alpha^\phi < 1$ is the relaxation factor for variable ϕ, ϕ'_p is the value of the state variable at node P to be used for the next iteration, ϕ^*_p is the value of the state variable at node P in the previous iteration, ϕ_{nb} are the values of the variables at the neighboring nodes and a_p, a_{nb}, and b are the constants from the discretized equation.

* Corresponding author.
E-mail addresses: jaina2@rpi.edu (A. Jain), kamind@rpi.edu (D.A. Kaminski).

0017-9310/$ - see front matter © 2009 Elsevier Ltd. All rights reserved.
doi:10.1016/j.ijheatmasstransfer.2009.03.019

Nomenclature

a_{nb}	coefficients for neighboring nodes in the discretized equation
a_P	coefficient of ϕ at node P in the discretized equation
A_f	amplitude of the harmonic with frequency f
A_f^*	normalized amplitude of the harmonic with frequency f
b	source term in the discretized equation
c_p	specific heat
Cr	conductance ratio
$e(n)$	error on iteration n
$\Delta e(n)$	change in error between iteration $n-1$ and n
f	frequency
g	acceleration of gravity
Gr	Grashof number, $Gr = \rho^2 g\beta(T_h - T_c)w^3/\mu^2$
H_f	discrete Fourier transform
H_o	Fourier transform at $f = 0$
k_f	thermal conductivity of the fluid
k_w	thermal conductivity of the wall
L	enclosure width
N	number of previous iterations over which the Fourier transform is taken
NB	"negative big"
NM	"negative medium"
NS	"negative small"
p_x	constant used in the membership functions, $p_x = 0.000893$
p_y	constant used in the membership functions, $p_y = 0.6329$
p_z	constant used in the weighting function and membership functions, $p_z = 27.785$
P	pressure of the fluid
P^*	effective pressure, $P^* = P + g\rho_c y$
PB	"positive big"
PM	"positive medium"
PS	"positive small"
q	applied heat flux
S^ϕ	magnitude of the solution vector for variable ϕ
$\overline{S}^\phi$	average magnitude of solution vector
t	thickness of the vertical wall
T	temperature
T_{amb}	ambient temperature
T_c	cold wall temperature
T_h	hot wall temperature
u	horizontal component of velocity vector
v	vertical component of velocity vector
w	height of the wall
W_f	weighting function for frequency f
x	coordinate in the horizontal direction
y	coordinate in the vertical direction

Greek symbols

α	relaxation factor
α^ϕ	relaxation factor for variable ϕ
β	volume expansivity
δ^ϕ	relative change in relaxation factor for variable ϕ
$\delta_c 1$	relative change in relaxation factor at the centroid of area 1
θ	inclination angle with respect to the vertical axis
μ	dynamic viscosity
μ_{mf}	value of the membership function
ρ	density of the fluid
ρ_c	reference density of the fluid
ϕ	generic symbol for the value of a state variable, either u, v, or T
ϕ_n	value of the state variable in the current iteration
ϕ'_n	value of the state variable to be used in the next iteration
ϕ_{n-1}	value of the state variable in the previous iteration
ϕ_{nb}	values of the state variables at the neighboring nodes
ϕ'_p	value of the state variable at point P to be used in the next iteration
ϕ^*_p	value of the state variable at point P from the previous iteration
ψ	non-dimensional temperature $\psi = (T - T_c)/(T_h - T_c)$

The present work deals with the computational fluid dynamics (CFD) investigation of laminar natural convection in enclosures with differentially heated conditions using fuzzy logic. The goal of the work is to find the limit where the controller algorithm fails to find a converged solution and compare this to the limit of convergence for fixed relaxation factors. Problems concerned with natural convection in enclosed cavities having conjugate heat transfer in one or more walls are investigated.

2. Problem analyzed

2.1. Problem 1 – Rectangular cavity with conjugate heat transfer in one wall

A schematic of the problem considered is shown in Fig. 1. The problem consists of a rectangular enclosure with isothermal boundary conditions at the extreme sides, i.e. cold (T_c) and hot wall (T_h) conditions at the left and right sides, respectively. The cavity is filled with a constant property fluid and the horizontal sides are insulated. Three walls of the enclosure are assumed to be of negligible wall thickness while the fourth, the right vertical wall, has a thickness t. The thickness ratio (t/L) is kept at 0.2. Because of the temperature gradient along the x direction, a buoyancy-driven recirculation pattern appears in the cavity. Firstly the conjugate heat transfer, i.e. the conduction through the thick walls, is analyzed by considering the conduction at the right side, i.e. hot-wall side only. The solid wall at the right side is simulated by substituting a very high value of the dynamic viscosity in the algorithm. The effect of wall conduction on natural convection flow in an enclosure was studied by Balvanz and Kuehn [12]; however, they considered the case of volumetric heat generation within

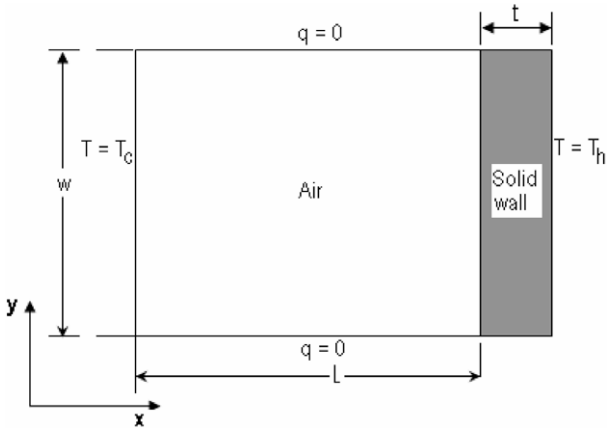

Fig. 1. Rectangular domain with conduction along the right wall.

the wall, and the outer face of the thick wall was taken to be insulated. Larson and Viskanta [13] accounted for wall conduction effects in an enclosed fire problem, but only one-dimensional wall conduction was considered. The problem definition and boundary conditions investigated in the present study are different from the above studies in that the conjugate effect is taken into account in two-dimensional analysis and for different sides as described in the later sections.

The flow was assumed to be Newtonian, incompressible, laminar, two-dimensional and steady. Viscous dissipation was neglected. All thermophysical properties were assumed constant and independent of the pressure and temperature fluctuations. However the density was treated using the Boussinesq approximation. The buoyancy force is in the y-direction.

The conservation equations for mass, momentum, and energy are given in Patankar [5] as

$$\frac{\partial u}{\partial x}+\frac{\partial v}{\partial y}=0$$

$$\rho\left(u\frac{\partial u}{\partial x}+v\frac{\partial u}{\partial y}\right)=-\frac{\partial P^*}{\partial x}+\mu\nabla^2 u$$

$$\rho\left(u\frac{\partial v}{\partial x}+v\frac{\partial v}{\partial y}\right)=-\frac{\partial P^*}{\partial y}+g\beta\rho(T-T_{amb})+\mu\nabla^2 v$$

$$\rho c_p\left(u\frac{\partial}{\partial x}(T-T_{amb})+v\frac{\partial}{\partial y}(T-T_{amb})\right)=k_f\nabla^2(T-T_{amb})$$

where P^* is an effective pressure given by

$$P^*=P+g\rho_c y$$

The velocity components at the boundaries are taken as zero. At the solid-liquid interface, the temperature and the heat flux must be continuous; this condition is mathematically expressed as

$$\left(\frac{\partial\psi}{\partial x}\right)_{fluid}=\frac{k_w}{k_f}\left(\frac{\partial\psi}{\partial x}\right)_{wall}$$

where ψ is the non-dimensional temperature given by

$$\psi=\frac{T-T_c}{T_h-T_c}$$

and k_w and k_f represent the thermal conductivities of wall and fluid, respectively.

The conservation equations listed above were discretized by a finite volume approach as defined by the following equation:

$$a_p\phi_p=\sum a_{nb}\phi_{nb}+b$$

where a_p is the coefficient for the point P under consideration, a_{nb}'s are the coefficients of neighboring grid points, ϕ_p is the value of the dependent variable for the equation under consideration, ϕ_{nb} 's are the values of the neighboring grid points and b is the source term. The generic variable ϕ is used to represent u, v, and T.

At every iteration, the assumed values of the solution vector were updated with under-relaxed values according to the following equation:

$$\phi'_n=\phi_{n-1}+\alpha^{\phi}(\phi_n-\phi_{n-1})$$

where α^{ϕ} is a relaxation factor for variable ϕ which varies between 0 and 1, ϕ'_n is the value of the state variable to be used for the next iteration n, ϕ_n is the value obtained from solution of the system of equations on iteration $n-1$, and ϕ_{n-1} is the value assumed before iteration $n-1$. Each of the two velocity components and the temperature are relaxed by separate relaxation factors. Thus, there are three relaxation factors specified on each iteration. Each relaxation factor is global and applies in every control volume over the entire domain. In the present algorithm due to Dragojlovic et al. [14], the controller adjusts the value of the relaxation factor based on the history of the solution curve for the last 50 iterations. At each iteration, the magnitude of the solution vector for variable ϕ is defined as

$$S^{\phi}(n)=\sqrt{\sum_{i=1}^{l}\sum_{j=1}^{m}[\phi_n(i,j)]^2}$$

where i and j are node numbers, l and m are the total number of nodes in the x and y directions, and ϕ_n is the value of variable ϕ on the n^{th} iteration. Exploratory calculations reported in Dragojlovic et al. [14] showed that some types of solution history curves converge quickly while others converge slowly or not at all. Generally, for low values of relaxation factor, the curve rises or falls monotonically or exhibits mild oscillations with a very slow rate of convergence. Somewhat higher relaxation factors produce oscillatory behavior with improved convergence. Raising the relaxation factor further increases the frequency and magnitude of the oscillations, while accelerating convergence. At some point, the oscillations become too pronounced and the convergence rate degrades. At very high relaxation factors, the solution history curve may oscillate on every iteration and either diverges or oscillates indefinitely.

Spectral analysis is applied to the solution history curve to identify desirable behavior. The number of previous iterations considered is N, where

$$N=n \quad \text{if } n<50$$

$$N=50 \quad \text{if } n\geqslant 50$$

and n is the current number of iterations in the simulation. The solution history curve can be treated as the discrete time representation of a signal. Taking a discrete Fourier transform on the data produces

$$H_f=\sum_{k=0}^{N-1}S_k^{\phi}e^{2\pi ikf}$$

where f is the frequency of the periodic components of the signal and

$$-\frac{1}{2}\leqslant f\leqslant\frac{1}{2}$$

The quantity i is the square root of -1. The Fourier transform is taken on each iteration for each of the three possible values of ϕ: u, v, and T.

The Fourier transform is used to identify how important particular harmonics are in the solution history curve. Only the frequencies that have physical meaning are included, so

$$0\leqslant f\leqslant\frac{1}{2}$$

When $f=0$, the corresponding harmonic does not oscillate at all and when $f=½$, the harmonic "zig-zags" on every iteration. The amplitude of the harmonic with frequency f is

$$A_f=\frac{2}{N}\sum_{k=0}^{N-1}S_k^{\phi}e^{2\pi ikf}=\frac{2}{N}H_f=a_f+ib_f$$

where a_f and b_f are the amplitudes of the cosine and sine functions, respectively. The amplitude of the harmonic is normalized by dividing it by the average magnitude of the solution vector. Using the values over the past N iterations, this average magnitude is

$$\bar{S}^{\phi}=\frac{1}{N}\sum_{k=0}^{N-1}S_k^{\phi}=\frac{1}{N}H_0$$

The normalized amplitude of the harmonic with frequency f is

$$A_f^*=\frac{|A_f|}{\bar{S}^{\phi}}=2\frac{\sqrt{\mathrm{Re}^2(H_f)+\mathrm{Im}^2(H_f)}}{H_0}$$

where Re and Im denote the real and imaginary parts of the Fourier transform.

As reported in Dragojlovic et al. [14], optimal convergence occurs just before the iteration becomes unstable. The onset of instability is heralded by the appearance of high-frequency harmonics with significant amplitude. The low frequency harmonics are desirable and accelerate convergence while the high frequency ones tend to drive the solution into divergence. The fuzzy controller is designed to keep high frequency harmonics at very low amplitudes while encouraging moderate amplitude low frequency harmonics.

To highlight the high frequency harmonics, an arbitrarily-defined weighting function is used:

$$W_f(f) = e^{\frac{p_z f}{f_{max}}}$$

where $f_{max} = ½$ is the maximum frequency of one cycle per two iterations. The constant $p_z = 27.785$ was chosen to optimize the performance of the controller for conjugate convection in a square cavity with $Gr = 10^6$, as described in Dragojlovic et al. [14].

The weighting function takes on low values at low frequencies and high values at high frequencies. The normalized amplitude of the harmonic is multiplied by the weighting function and the result is compared with unity. The desired goal is to keep this product near unity, i.e.

$$W_f(f)A_f^* \approx 1$$

If $W_f(f)A_f^*$ is much less than unity, then all frequencies are suppressed and convergence is very slow. We would like to encourage the low frequency harmonics, while limiting the high frequencies. If $W_f(f)A_f^* \approx 1$, the low frequencies have significant amplitude and the high frequencies are limited. If $W_f(f)A_f^*$ is much greater than unity, the high frequencies are too prominent and divergence is likely.

The task of selecting a relaxation factor is formulated as a control problem. We define the error on iteration n as

$$e(n) = \ln(\max[W_f(f)A_f^*])$$

The argument of the logarithm is the maximum weighted amplitude of all the frequencies in the solution history. When the largest weighted amplitude is near unity, the error becomes zero.

The fuzzy rules are formulated in terms of the error and the change in error. The change in error from one iteration to the next is simply defined as

$$\Delta e(n) = e(n) - e(n-1)$$

Fuzzy logic is a technique for expressing uncertain linguistic variables such as "big" and "small" into quantifiable values that can be used to make decisions. In this case, we express the error as "negative big (NB)," "negative medium (NM)," negative small (NS)," "positive small (PS)," "positive medium (PM)," or "positive big (PB)." The degree to which an error falls into a particular category is computed with the triangular input membership functions shown in Fig. 2. The function PS is the downward sloping line defined over the domain from 0 to $p_y p_z$ on the abscissa; PM is a triangular function defined from 0 to p_z and PB is two continuous line segments defined from $p_y p_z$ to infinity. The degree of membership, plotted along the ordinate, takes on the value 1 if the error is most certainly in that category and the value zero if the error is definitely not in that category. Values between 0 and 1 are used to quantify how well an error fits in a particular category. An error can fit in two categories simultaneously. For example, if the value of the error is $(p_y p_z + p_z)/2$, the PM function returns 0.5 and the PB function also returns 0.5. This is equivalent to a panel of human experts in which half of them decide that the error is positive medium and half decide it is positive big, but no one chooses positive small.

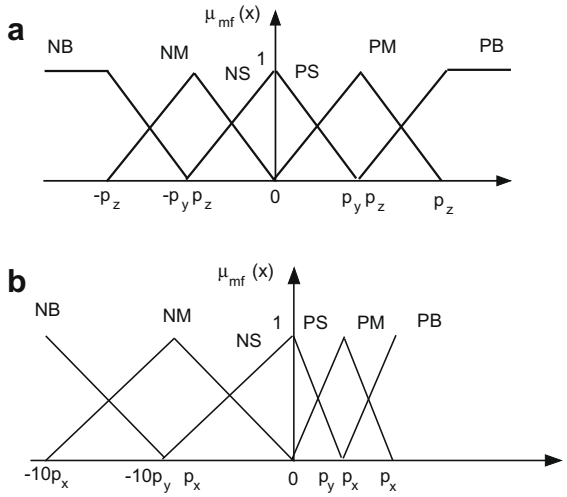

Fig. 2. (a) Input membership functions, (b) output membership functions: $p_x = 0.000893$, $p_y = 0.6329$, $p_z = 27.785$.

The input functions are used to categorize the size of the error and the change in error. Then a fuzzy rule set is used to determine the appropriate action that the algorithm should take. In this case, actions are changes in the relaxation factors for the variable in question (either u, v, or T). The output variables determined by the control system are the relative changes in relaxation factors defined as

$$\delta^{\phi}(n) = \frac{\Delta\alpha^{\phi}(n)}{\alpha^{\phi}(n)} = \frac{\alpha^{\phi}(n) - \alpha^{\phi}(n-1)}{\alpha^{\phi}(n)}$$

where $\alpha^{\phi}(n)$ is the relaxation factor for the variable ϕ at the n^{th} iteration.

The fuzzy rule set includes the rules detailed in Table 1. Each cell in the table represents one rule. For example, one rule is

IF *the error* $e(n)$ *is* ***negative small AND*** *the change in error* $\Delta e(n)$ *is* ***negative medium***
THEN *the change in the relaxation factor* $\delta^{\phi}(n)$ *is* ***positive medium***

If the error is small, we are probably close to convergence; if the change in error is negative medium, the error is smaller than it was on the last iteration and we are approaching convergence at a good rate. This implies that we may be able to increase the relaxation factor to drive the simulation to converge more rapidly. The other rules in Table 1 also adjust relaxation factors to either increase or decrease based on heuristic reasoning about what is likely to improve convergence or avoid divergence.

The application of the sample rule is illustrated in Fig. 3. At a particular iteration, the error $e(n)$ falls within the category "negative small (NS)", and the degree of membership is 0.3. As a result, we "fill up" the output membership function, PM, to the height 0.3, as shown by the shaded area in Fig. 3. The change in error falls

Table 1
The *error* is listed to the left of the table and the *change in error* below the bottom of the table. Cells in the table represent the output fuzzy set that results from the size of the *error and the change in error*.

PB		NS	NM	NM	NB	NB
PM	PS		NS	NM	NM	NB
PS	PM	PS		NS	NM	NM
NS	PM	PM	PS		NS	NM
NM	PB	PM	PM	PS		NS
NB	PB	PB	PM	PM	PS	
	NB	NM	NS	PS	PM	PB

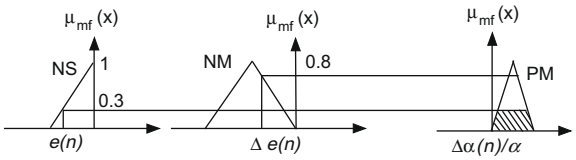

Fig. 3. Example of application of a fuzzy rule.

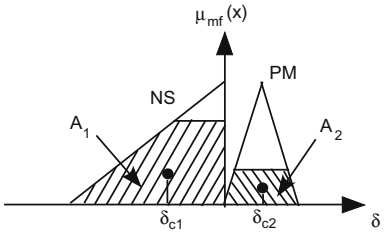

Fig. 4. Defuzzification of the output signal.

within the category NM to the height 0.8. We consider the area of the output PM filled to the height 0.8. We then choose the smaller of the two output areas, which is the shaded area. We say that the rule has "fired" and produced an output area.

More than one rule may fire on a given iteration. For example, the value of the error in Fig. 3 fits in the category NM as well as in the category NS. If multiple rules fire, several different areas may result in the output. Fig. 4 shows a sample result from two rules firing. The quantities δ_{c1} and δ_{c2} are the x components of the centroids of areas A_1 and A_2, respectively. In this case one rule is suggesting a PM change in relaxation factor and the other a NS change, as if one expert were saying "raise it somewhat" and the other were saying "lower it a bit". To decide on a final "crisp" value, the area-weighted average of the two δ values is used, i.e.

$$\delta^{\phi}(n) = \frac{\Delta\alpha^{\phi}(n)}{\alpha^{\phi}(n)} = \frac{A_1\delta_{c1} + A_2\delta_{c2}}{A_1 + A_2}$$

Note that the positive changes in relaxation factor (raising it) are much smaller than the negative ones (lowering it). The output membership functions in Fig. 2b extend 10 times farther along the negative x-axis than along the positive x-axis. It is essential that divergence be avoided, so aggressive reductions in relaxation factor are useful. On the other hand, even when the simulation is rather close to convergence, a stiff simulation can be tipped into instability by even a mild increase in relaxation factor. The values of p_x, p_y, and p_z used here give optimal performance for the case of conjugate convection in one wall at $Gr = 10^6$.

The program begins execution with all relaxation factors set to a default value of 1. The rule set is applied on every iteration. If divergence occurs, which is recognized when computed values hit the machine limit, the program automatically restarts with relaxation factors that are 10% lower. When magnitudes of the residual vectors are increasing, positive increments in relaxation factors called for by the fuzzy rules are ignored. After the increment in relaxation factor is defuzzified, the relaxation factor is updated by

$$\alpha(n+1) = \alpha(n) + \Delta\alpha(n)$$

The validity of the fuzzy logic algorithm was first tested with the benchmark problem similar to the one discussed above but with the conductance ratio (Cr) of 1.0 as done in [14–16]. The conductance ratio is defined as

$$Cr = \frac{k_w L}{k_f t}$$

Table 2
Comparison of fuzzy logic algorithm with benchmark problem.

Gr	C_{ratio}	Liaqat and Baytas [15], Nu	Kaminski and Prakash [16], Nu	Present Nu
10^3	1.0	0.877	0.87	0.865
10^5	1.0	2.082	2.08	2.09
10^7	1.0	2.843	2.87	2.859

where k_w and k_f are the thermal conductivities of the solid wall and fluid, respectively. Table 2 shows the comparison of the results with the benchmark results for different values of Grashof number.

The grid size used for the rectangular domain was 40×34. Out of the 40 vertical grid lines used for discretizing the x-axis, a disproportionate share of 10 grid lines were used for simulating the solid wall conditions. The grid was packed close to the solid walls and the solid-fluid interface so that the boundary layer could be well resolved. The wall was modeled as a fluid of very high viscosity. The grid layout was chosen after a number of trial numerical experiments, the results of which were summarized in [16]. The rectangular enclosure was considered for different tilt angles, i.e. the inclination of the acceleration due to gravity with respect to the vertical axis. Three different values of tilt angle $\theta = 0°$, 45°, and 80° are analyzed. Cr was varied from 0.01 to 100.

Table 3 shows the number of iterations required with different constant relaxation factors and with the controller algorithm for inclination angles of $\theta = 0°$, 45°, and 80°, respectively, at $Cr = 0.01$. For all the inclination angles it was found that the controller was able to find a converged solution for higher values of Grashof number as compared to the best constant relaxation factor. At

Table 3
Number of iterations at different Grashof numbers for varying relaxation factors and the controller algorithm for $Cr = 0.01$.

Gr	Relaxation factor				
	0.1	0.3	0.6	0.9	Controller
$Cr = 0.01$, $\theta = 0°$					
10^7	17850	4748	1526	670	874
2×10^7	16525	4331	1661	div	796
3×10^7	15768	4150	1900	div	736
4×10^7	15253	4182	div	div	724
8×10^7	14235	4865	div	div	1132
10^8	14048	div	div	div	div
10^9	div	div	div	div	7462
10^{10}	div	div	div	div	5420
10^{11}	div	div	div	div	5655
10^{12}	div	div	div	div	9726
10^{15}	div	div	div	div	div
10^{20}	div	div	div	div	div
$Cr = 0.01$, $\theta = 45°$					
10^7	19817	5361	1806	629	479
4×10^7	18744	div	1990	div	840
8×10^7	19138	div	div	div	1132
10^8	19419	div	div	div	1119
10^9	div	div	div	div	8332
10^{10}	div	div	div	div	2387
10^{11}	div	div	div	div	div
10^{12}	div	div	div	div	div
10^{15}	div	div	div	div	div
$Cr = 0.01$, $\theta = 80°$					
10^7	25882	6490	1902	502	547
4×10^7	26086	6498	2189	div	670
8×10^7	27571	div	div	div	1204
10^8	26571	div	div	div	39495
10^9	div	div	div	div	2285
10^{10}	div	div	div	div	5259
10^{11}	div	div	div	div	6881
10^{12}	div	div	div	div	div
10^{13}	div	div	div	div	div

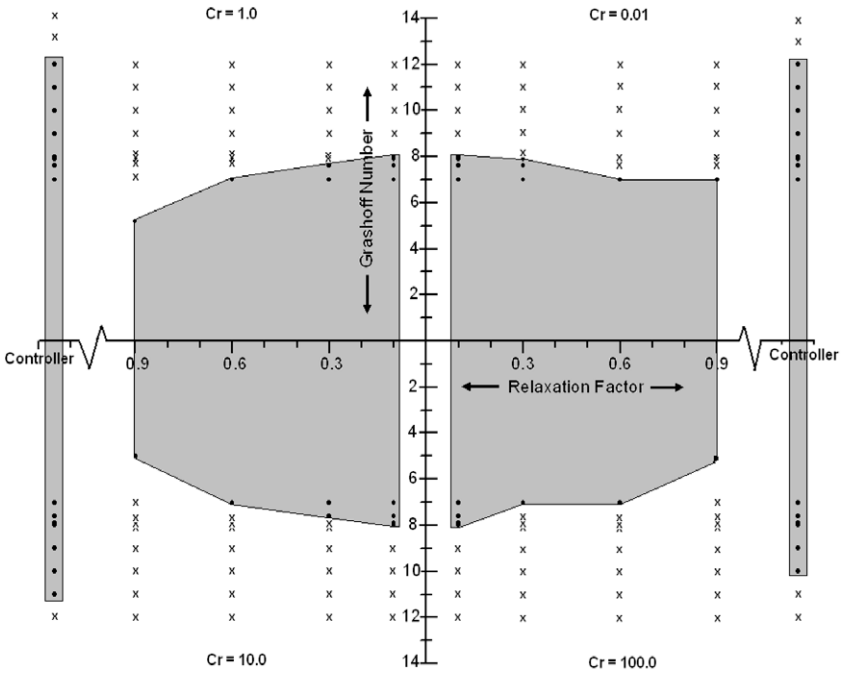

Fig. 5. Comparison of zones of convergence for Problem 1 with fixed relaxation factors and variable (controlled) relaxation factors, $\theta = 0^\circ$ (dots represent converged solutions and crosses represent divergence).

the no-inclination case, the controller found a converged solution until $Gr = 10^{12}$; for inclination angles of 45° and 80°, the Grashof number limits are $Gr = 10^{10}$ and $Gr = 10^{11}$, respectively. The constant relaxation factors were never able to find a converged solution above $Gr = 10^8$. In the case of low constant relaxation factors, such as 0.1, divergence probably occurs because round-off errors accumulate faster than solution corrections converge. In addition, low relaxation factors typically lead to a large number of iterations. Increasing the inclination angle of the enclosed cavity increases the degree of complexity and makes convergence less likely.

For higher values of Cr ($Cr = 1.0$) and at $\theta = 80^\circ$ the constant relaxation factor fails to find a converged solution even for lower values of Grashof number. Divergence is defined as the condition when the algorithm fails to find a converged solution in 100,000 iterations. However the fuzzy controller algorithm found a converged solution up to $Gr = 10^{10}$. For $Cr = 10.0$ and $\theta = 80^\circ$ this value was $Gr = 10^{12}$. Also at $\theta = 80^\circ$ the controller algorithm outperformed the constant relaxation factors case. Thus at higher values of Cr (= 1.0, 10.0 and 100.0) and at $\theta = 80^\circ$ the constant relaxation factors had difficulty in finding a converged solution; however, the controller was limited by $Gr = 10^{10}$, 10^{12} and 10^9 for $Cr = 1.0$, 10.0 and 100.0, respectively.

Fig. 5 shows a graphical representation of the zone of convergence for different values of Cr at $\theta = 0^\circ$ for the given problem. The relaxation factor and the controller are plotted on the x-axis while the logarithmic scale for Grashof number is used in the y-axis. The dots represent converged solutions and the x's represent divergence. The shaded region represents the zone of convergence for different Cr. As seen the zone is considerably extended when using the controller algorithm.

At higher values of Grashof number, the flow may not remain laminar. In the actual physical domain, small disturbances are accentuated and turbulence develops. In the numerical simulation, the problem becomes more and more ill-conditioned as the Grashof number becomes larger. One advantage of the controller is that it can solve such ill-conditioned cases, i.e., cases where small changes in the input lead to large changes in the output.

2.2. Problem 2 – Rectangular cavity with conjugate heat transfer in two side walls

The membership functions were optimized for natural convection in a square enclosure with one conjugate wall. We now explore their application in a similar geometry, one with two walls, to identify the zone of convergence. (see Fig. 6). The boundary conditions are maintained the same.

Figs. 7 and 8 show the graphical representation of the zone of convergence for different values of Cr at $\theta = 0^\circ$ and $\theta = 45^\circ$, respectively. When using the controller algorithm the range of shaded region is increased showing the efficacy of the algorithm. Interestingly, when the enclosure is tilted at 45° for $Cr = 0.01$, no constant value of relaxation factor was found that produced convergence for $Gr = 10^7$. However, the controller was able to achieve convergence for $Gr = 10^9$ in a small number of iterations (=2201). The controller operates by selecting small values of relaxation factor early in the

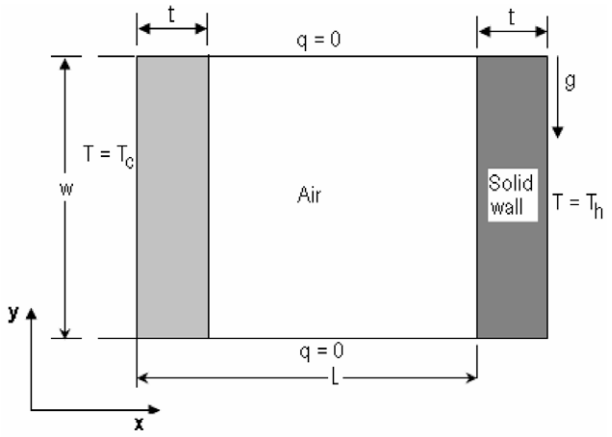

Fig. 6. Rectangular domain with conduction in two side walls.

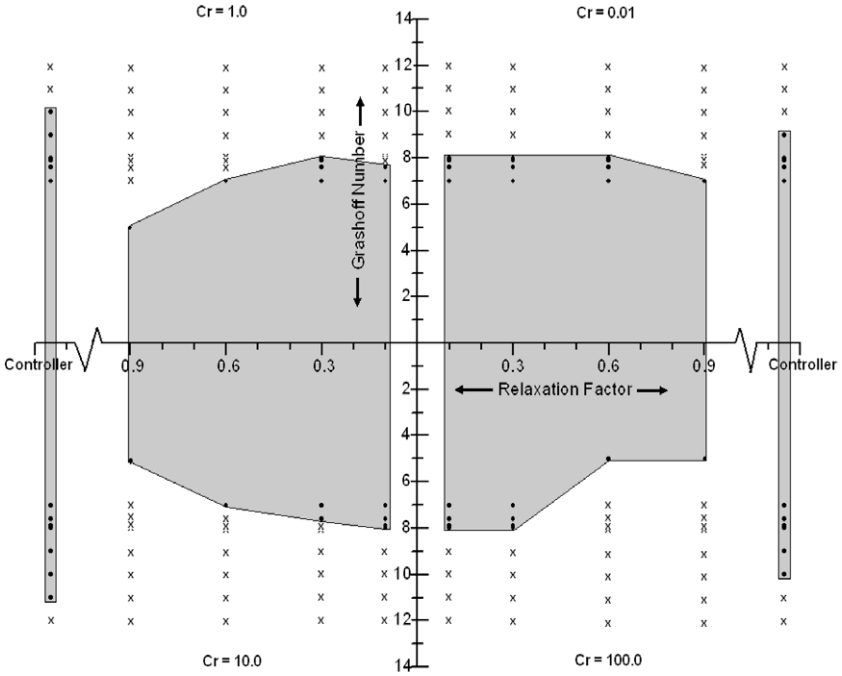

Fig. 7. Zones of convergence for Problem 2 with fixed relaxation factors and variable (controlled) relaxation factors, $\theta = 0$.

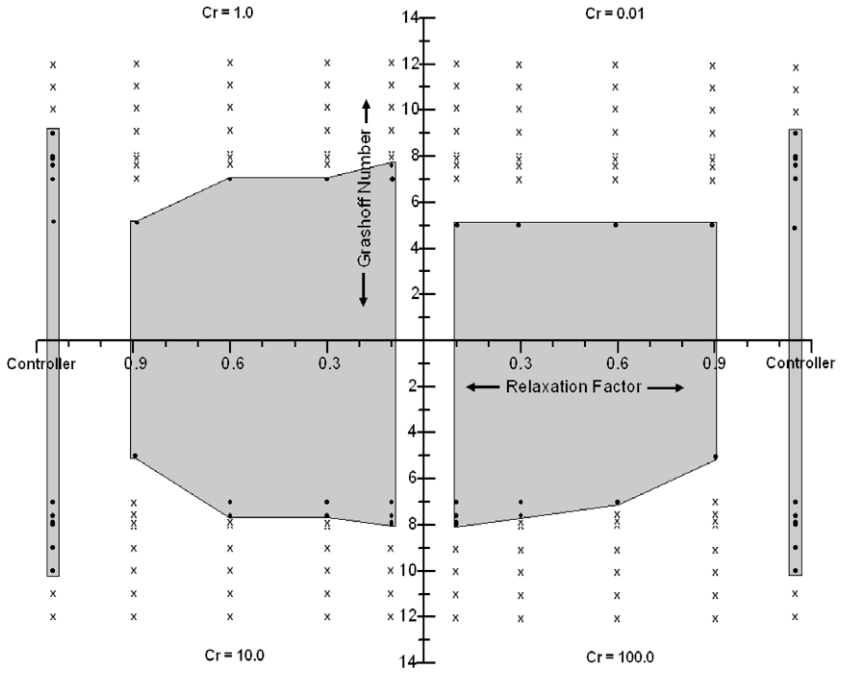

Fig. 8. Zones of convergence for Problem 2 with fixed relaxation factors and variable (controlled) relaxation factors, $\theta = 45°$.

iteration to avoid oscillatory divergence and then using larger values later in the iteration to avoid round-off error induced divergence. The constant relaxation factors fail due to one or the other effect.

2.3. Problem 3 – Rectangular cavity with conjugate heat transfer in three walls

This problem considers conjugate heat transfer in three walls, two side walls and the bottom wall, as shown in Fig. 9, the boundary conditions are maintained the same. Also the thickness of the walls is the same.

Fig. 10 shows the graphical representation of the zone of convergence for different values of *Cr* at $\theta = 80°$ for the given problem. Constant relaxation factors of 0.6 and 0.9 were not able to find a converged solution for $Gr = 10^7$ at all the values of *Cr*. A value of 0.1 as the relaxation factor increased the area of convergence but was limited by $Gr = 10^8$.

2.4. Problem 4 – Rectangular cavity with conjugate heat transfer in all the walls

This problem involves conjugate heat transfer in all four walls. The boundary conditions are the same as described for the above

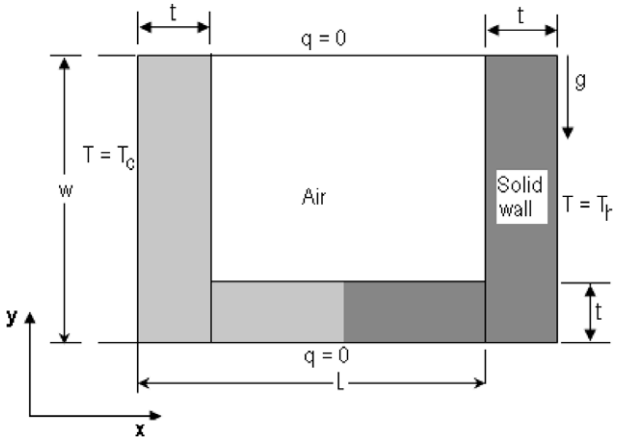

Fig. 9. Rectangular domain with conduction in three walls.

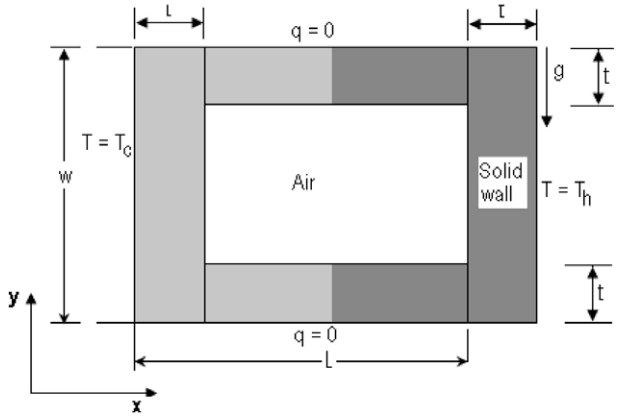

Fig. 11. Rectangular domain with conduction in all the walls.

cases. Also, an equal number of grid lines were used to discretize all the four walls. Fig. 11 shows the problem under consideration. There is a temperature gradient from the left wall (at lower temperature) to the right wall (at higher temperature).

Fig. 12 shows the graphical representation of the zone of convergence for different values of Cr at $\theta = 80^\circ$ for the given problem. For $Cr = 0.01$, 1.0 and 10.0 all the constant relaxation factor values (=0.1, 0.3, 0.6 and 0.9) were not able to find a converged solution for $Gr = 10^7$, however, the controller extended the zone of convergence till $Gr = 8 \times 10^7$, 10^{11} and 10^{11}, respectively. For $Cr = 100.0$ the relaxation factor values of 0.1 and 0.3 increased the convergence region till $Gr = 10^8$ however the same behavior was observed for the 0.6 and 0.9 values of relaxation factor. The controller however found a converged solution till $Gr = 10^{12}$.

3. Probability of convergence

Another way to view the efficacy of the controller for problems of the type studied here is to define a "probability of convergence" as the number of cases which converged divided by the total number of simulations attempted. To find the true value of this probability, an infinite number of cases would have to be considered. However, a reasonable estimate of the probability can be determined by examining a large number of cases. In this investigation, a total of 2400 cases were considered.

The probability of convergence for all the problems studied at $\theta = 0^\circ$, 45° and 80° are shown in Figs. 13–15 respectively. At $\theta = 0^\circ$ and 45° the probability of convergence was much better for the controller algorithm than for the constant cases. The 0.1 constant relaxation factor showed 100% convergence probability till 4×10^7 for at $\theta = 0^\circ$ after which the probability decreased until at $Gr = 10^9$ it was 0. For higher values of relaxation factor there was a rapid decline in the convergence probability with increasing values of Grashof number.

For $\theta = 80^\circ$ the probability of convergence with fixed relaxation factors was zero after $Gr = 10^9$. However the controller showed some non-zero probability until $Gr = 10^{12}$. On the other hand, the probability was less than 50% for any of the constant relaxation factors.

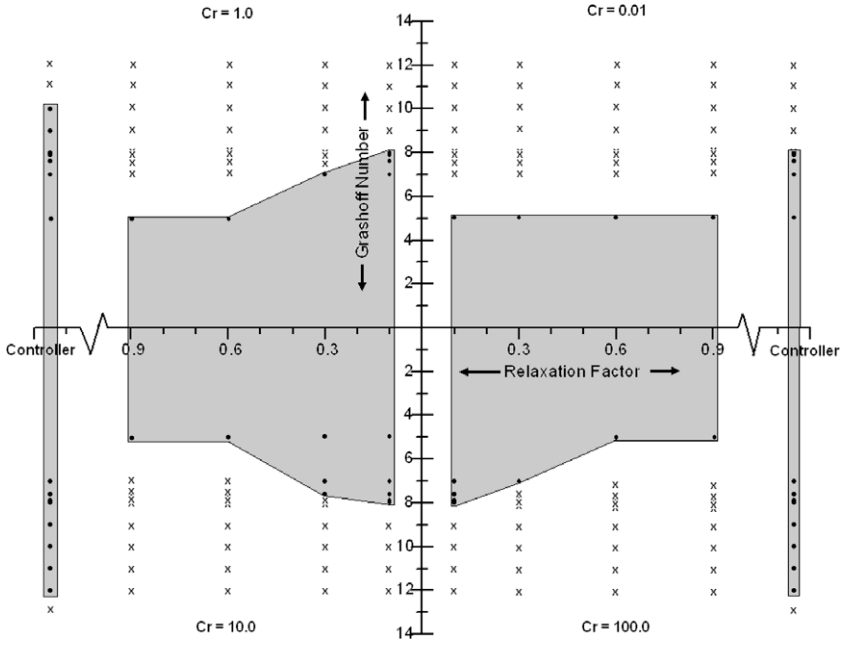

Fig. 10. Zones of convergence for Problem 3 with fixed relaxation factors and variable (controlled) relaxation factors, $\theta = 80^\circ$.

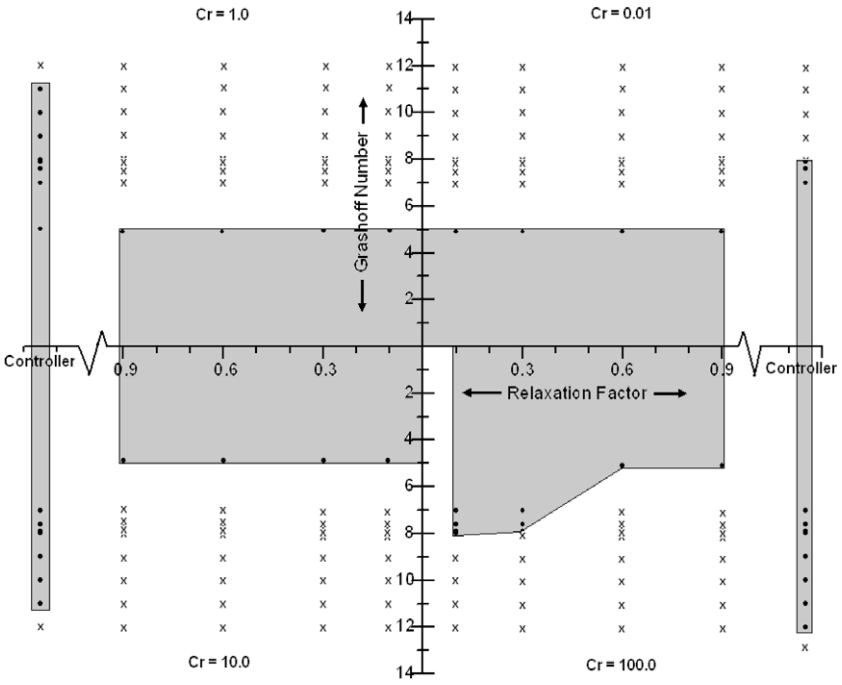

Fig. 12. Zones of convergence for Problem 4 with fixed relaxation factors and variable (controlled) relaxation factors, $\theta = 80°$.

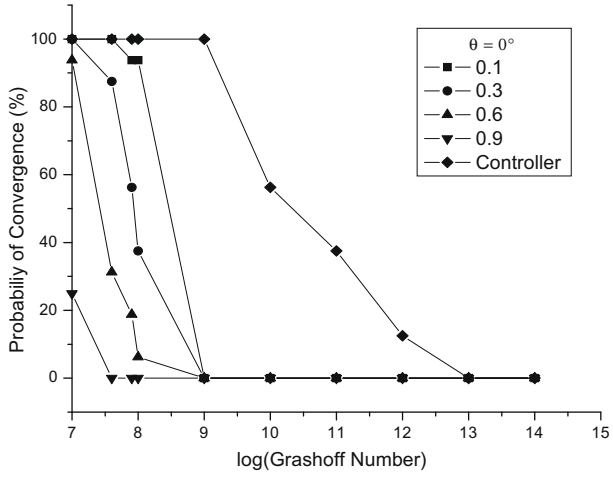

Fig. 13. Probability of convergence at different Grashof number for $\theta = 0°$.

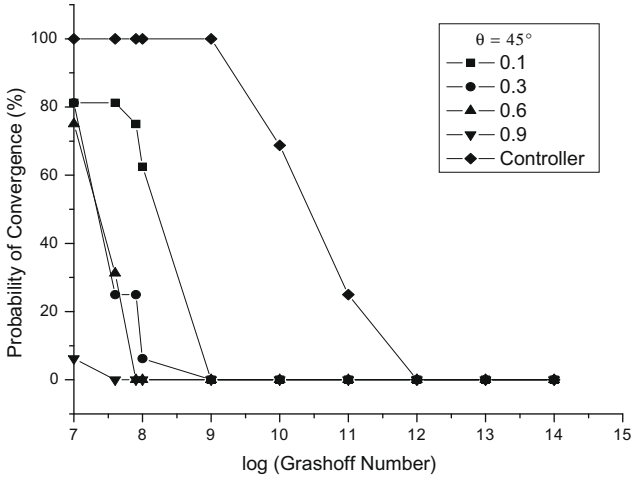

Fig. 14. Probability of convergence at different Grashof number for $\theta = 45°$.

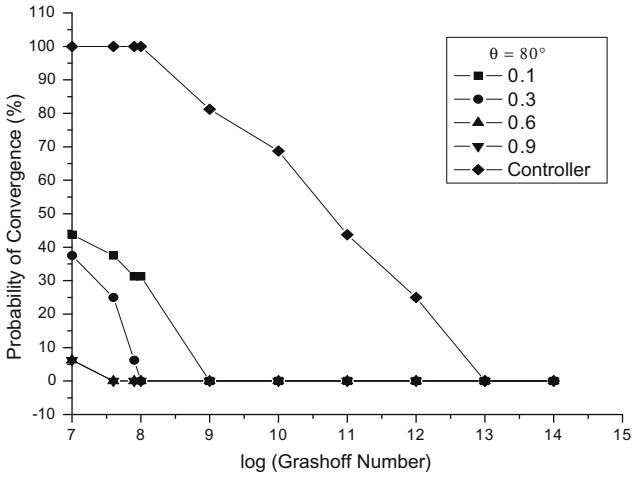

Fig. 15. Probability of convergence at different Grashof number for $\theta = 80°$.

4. Conclusions

The present work investigates the limits of convergence for laminar natural convection in enclosed cavities with conjugate heat effects applied to different walls of the cavity. The controller algorithm using a fuzzy set of rules outperformed the manual relaxation factors in all the cases studied. It is reasonable to expect that when fuzzy logic is used to adjust relaxation factors in other CFD simulations, convergence will be enhanced. The decision making system was based on monitoring the behavior of characteristic computational parameters and applying a fuzzy set of rules with pre-defined membership functions in order to tune the relaxation factors in a direction which provides the best speed of convergence. The controller is not limited to this geometry or physical condition, but is generally applicable to a wide variety of situations, as shown by Dragolovic et al. [17]. It is expected that the controller will extend the range of convergence in other simulations as it does in this case.

References

[1] I. Catton, Natural convection in enclosures, in: Proceedings of 6th International Heat Transfer Conference, vol. 6, 1978, pp. 13–31.
[2] B. Gebhart, Y. Jaluria, R.P. Mahajan, B. Sammakia, Buoyancy-induced Flows and Transport, Hemisphere, New York, 1988.
[3] S. Ostrach, Natural convection in enclosures, Adv. Heat Transfer 8 (1972) 161–227.
[4] S. Ostrach, Natural convection heat transfer in cavities and cells, in: Proceedings of 7th International Heat Transfer Conference, Munich, F.R.G., vol. 1, 1982, pp. 365–379.
[5] S.V. Patankar, Numerical Heat Transfer and Fluid Flow, Series in Computational Process and Thermal Sciences, Hemisphere, Washington, DC, 1980.
[6] Z. Dragojlovic, D.A. Kaminski, J. Ryoo, Tuning of a fuzzy rule set for controlling convergence of a CFD solver in turbulent flow, Int. J. Heat Mass Transfer 44 (2001) 3811–3822.
[7] S. Iida, K. Ogawara, S. Furusawa, N. Ohata, A fast converging method using wobbling adaptive control of SOR relaxation factor for 2D Benard convection, J. Mech. Eng. Soc. Jpn. 7 (1994) 168–174.
[8] M. Srinivas, L.M. Patnaik, Adaptive probabilities of crossover and mutation in genetic algorithms, IEEE Trans. Syst. Man Cybern. 24 (4) (1994) 656–667. Aug.
[9] P.T. Wang, G.S. Wang, Z.G. Hu, Speeding up the search process of genetic algorithm by fuzzy logic, in: Proceedings of 5th Eur. Congr., Intelligent Techniques and Soft Computing, 1997, pp. 665–671.
[10] R. Subbu, A.C. Sanderson, P.P. Bonissone, Fuzzy logic controlled genetic algorithm versus tuned genetic algorithm: an agile manufacturing application, in: Proceedings 1999 IEEE Int. Symp. Intelligent Control (ISIC), 1998, pp. 434–440.
[11] L. Xunliang, T. Wenquan, Z. Ping, H. Yaling, W. Qiuwang, Control of convergence in computational fluid dynamics simulation using fuzzy logic, Sci. China Ser. E–Technol. Sci. 45 (5) (2002) 495–502.
[12] J.L. Balvanz, T.H. Kuehn, Effect of wall conduction and radiation on natural convection in a vertical slot with uniform heat generation on the heated wall, in: K. Torrance, I. Catton (Eds.), Natural convection in enclosures, vol. 8, ASME HTD, 1980, pp. 163–174.
[13] D.W. Larson, R. Viskanta, Transient combined laminar free convection and radiation in a rectangular enclosure, J. Fluid Mech. 44 (1984) 153–176.
[14] Z. Dragojlovic, D.A. Kaminski, J. Ryoo, Tuning of membership functions in a fuzzy rule set for controlling convergence of laminar CFD solutions, in: Proceedings of 2001 ASME IMECE, HTD-24288, 2001.
[15] A. Liaqat, A.C. Baytas, Conjugate natural convection in a square enclosure containing volumetric sources, Int. J. Heat Mass Transfer 44 (2001) 3273–3280.
[16] D.A. Kaminski, C. Prakash, Conjugate natural convection in a square enclosure: effect of conduction in one of the vertical walls, Int. J. Heat Mass Transfer 29 (12) (1986) 1979–1988.
[17] Z. Dragojlovic, D. A. Kaminski, J. Ryoo, Control of convergence in convective flow simulations using a fuzzy rule set that stabilizes iterative oscillations, in: Proceedings of the 33rd National Heat Transfer Conference, Albuquerque, NM, 1999.